

PASSIVE CHARGING OF A SOLAR HEAT STORAGE SYSTEM

Reynaldo C. Castro

Division Chief III

Products Development and Waste Utilization Division

National Tobacco Administration

Main Research Center

Batac 2906 Ilocos Norte

John G. Alphin

Professor

Pee Dee Research and Education Center

Florence, SC, USA

William H. Allen

Professor

Department of Biological and Agricultural Engineering

Clemson University, Clemson, SC, USA

ABSTRACT

A computer simulation model using the performance equation of a vortex machine obtained under laboratory conditions was developed and used to predict the performance of this device in passively charging a solar heat storage system. Based on the results, the vortex machine can theoretically be used as an effective charging device.

Introduction

Passive solar energy systems are not as efficient as active ones. The inefficiencies are mainly due to the difficulties associated with charging and discharging the heat storage medium. In a natural convection solar tobacco curing system developed by Castro et al. (1985), for example, the contribution of the rockbed heat storage was minimal. Similarly, Vered and Sebald (1981) observed difficulties in discharging the heat stored in a passive rock bin in their solar house studies. In both, the need for a way to effectively circulate the air passing through the rockbed was recognized.

A novel approach to alleviate this problem without resorting to energy-consuming and expensive blowers is to use wind-aided passive airflow inducers. In this study, the performance of a vortex machine to induce airflow and aid in charging a rockbed

heat storage was investigated by computer simulation. The objectives of this simulation were:

1. To explore the feasibility of using vortex machines as passive charging devices for a rockbed heat storage system, and
2. to develop a computer simulation model to predict the performance of such a system.

Methodology

The System

System description. The simulated system was part of an integrated solar- and wind- aided tobacco curing barn (Figure 1). Its main components were the solar collectors, the rockbeds, the curing chamber and the vortex machines. The barn was oriented with its solar collector walls facing north-south.

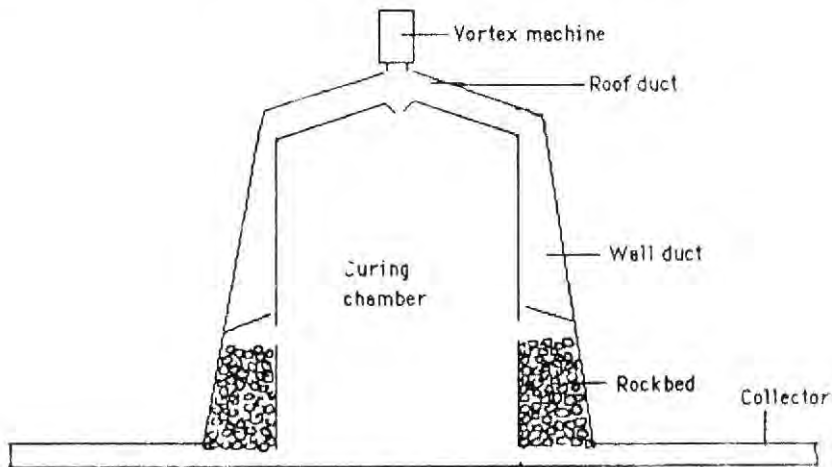


Figure 1. The integrated solar - and wind-aided tobacco curing barn.

The solar collectors had a total area of 64 m^2 and had a width of 8 m and length of 4 m. A 0.15 m clearance between the absorber and the single glass cover served as the air duct. A collector efficiency of 85% and heat loss coefficient of 8 W/m^2 was assumed. These are typical values for a single cover air-type flat plate collector (Duffie and Beckman, 1980).

The rockbeds had a total flow area of 8 m^2 and were 1 m deep. The rocks were assumed to have an average diameter of 20 mm and void fraction of 0.4.

The curing chamber measured $8 \times 4 \times 4 \text{ m}$, giving a volume enough to accommodate the produce from a half-hectare tobacco field.

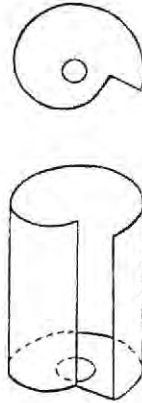


Figure 2. The vortex machine used in the study .

The vortex machine model (Figure 2) is similar to the optimum configuration of a spiral-type vortex machine found by Yen (1980). It was constructed of lexan and with a diameter of 25.4 cm and height of 50.8 cm. The spiral shape of the wall is given by

$$r = r_o \exp(0.1\Theta)$$

where r is the radius and r_o is 12.7 cm.

To increase the airflow further, the outer walls and roof were assumed painted flat black. The walls and roof, therefore, acted as bare solar collectors plates which increased the temperature of the exiting air and, consequently, the potential draft.

Sytem operation. Heated air from the solar collectors was caused to flow through the rockbeds by the combined actions of thermal bouyancy and suction force created by the vortex machine. As the heated air passed through the rockbed, most of its heat was transferred to the rocks. In the process, the rockbed was charged while the air temperature dropped. The air was reheated by the solar energy absorbed by the walls and roof to increase the draft. Finally, the air exited through the vortex machines.

System equations. The main motive force in the system came from the suction generated by the vortex machine. It was supplemented by the "stack effect" resulting from the differences in the densities of the solar heated and ambient air. These forces interacted with frictional and other losses in the system to create a steady-state condition of flow. Converting these forces into their equivalent pressure heads facilitates the use of the Bernoulli equation in analyzing the resulting airflow. The equation has the form

$$P + (pV^2/2) + hz = \text{constant} \quad (1)$$

where the left side terms represent pressure, kinetic and potential fluid energies and the variables are

p = static pressure, Pa,
 ρ = density of the ambient air, kg/m^3 ,
 V = ambient wind velocity, m/s, and
 h = elevation, m.

The suction pressure developed by the vortex machine, ΔP_{vm} , was found by Castro (1991) to follow the equation

$$(\Delta P_{vm} = 4.903(\rho V^2/2)) \quad (2)$$

On the other hand, the thermal draft generated by the system is

$$(\Delta P_{th} = g\{H_c \sin B(\rho_{amb} - \rho_c) + H_{wd}(\rho_{amb} - \rho_{wd}) + H_r(\rho_{amb} - \rho_r)\}) \quad (3)$$

where

ΔP_{th} = suction pressure due to thermal effects, Pa,
 g = acceleration due to gravity (9.8 m/s^2),
 h_c = height of the solar collector duct, m,
 B = slope of the solar collector, deg,
 H_{wd} = height of the wall duct, m, and
 H_r = height of the roof, m.

The subscripts amb, c, wd and r denote ambient, collector, wall duct and roof duct conditions, respectively.

The vortex suction and thermal draft must be able to generate the velocity pressure and overcome frictional lossess. These pressure drops are as follows:

velocity

$$\Delta P_{vc} = \rho V^2/2; \quad (4)$$

collector (Shewen and Hollands, 1978)

$$\Delta P_c = \rho f Q^2 (1_c/b)^3; \quad (5)$$

rockbed (Dunkle and Ellul, 1972)

$$\Delta P_{rb} = H_{rb} G^2 / \rho D_r (21 + 1750 u/GD_r); \quad (6)$$

wall duct

$$\Delta P_{\text{wd}} = (1 + f(L_{\text{wd}}/D_{\text{h,wd}})) \rho V^2/2; \quad (7)$$

roof duct

$$\Delta P_{\text{rd}} = (1 + f(L_{\text{rd}}/D_{\text{h,rd}})) \rho V^2/2; \quad (8)$$

where f , the friction factor, can be computed as

$$f = 0.1335 \text{Re}^{-0.317} \quad (9)$$

for the typical operating range of Reynolds numbers, 2,000 to 10,000 (Shewen and Hollands, 1978). The nomenclatures in the above equations are

P	=	pressure, Pa,
Q	=	volumetric flow rate per unit collector area, $\text{m}^3/(\text{s m}^2)$,
G	=	mass flow rate per unit area of rockbed, $\text{kg}/(\text{s m}^2)$,
L	=	length, m
b	=	collector duct height, m,
H	=	depth of rockbed, m,
D_r	=	average rock or pebble diameter, mm, and
D_h	=	hydraulic diameter, m.

The subscripts vel, c, rb, r, wd, and rd refer to velocity, collector, rockbed, rock, wall duct and roof duct, respectively.

In addition, the system also has two bends as indicated in Figure 1. The corresponding losses in these bends are

$$\Delta P_{\text{bend1}} = (1 + 1.2) \rho_c V^2/2 \quad (10)$$

$$\Delta P_{\text{bend2}} = (1 + 1.25 (30/90)^2) \rho_{\text{wd}} V^2/2 \quad (11)$$

with each term as previously defined.

In the above equations, the pressure loss in the rockbed (Equation 6) is expressed in terms of the massflow rather than velocity. This is desirable since massflow remains constant, regardless of changes in temperature or pressure, while velocity varies accordingly. Expressing the other pressure drops in terms of massflow, therefore, gives the following equations which implicitly satisfy the continuity requirement:

$$\Delta P_{\text{vel}} = P_{\text{amb}} (m/p_{\text{amb}} A_{\text{xc}})^2/2 \quad (12)$$

$$\Delta P_c = P_c f (m/p_c A_c)^2 (L_c/b)^3 \quad (13)$$

$$\Delta P_{wd} = (1 + f(L_{wd}/D_{h,wd})) P_{a,wd} (m/A_{x,wd} P_{wd})^2 / 2 \quad (14)$$

$$\Delta P_{rd} = (1 + f(L_{rd}/D_{h,rd})) P_{a,rd} (m/A_{x,rd} P_{rd})^2 / 2 \quad (15)$$

$$\Delta P_{bend1} = (1 + 1.2) P_{a,c} (m/A_{x,wd} P_{wd})^2 / 2 \quad (16)$$

$$\Delta P_{bend2} = (1 + 1.25(30/90)) 2 P_{a,wd} (m/A_{x,wd} P_{wd})^2 / 2 \quad (17)$$

where

m = massflow, kg/s,

A_x = cross sectional area normal to flow, m^2 , and the other parameters as previously defined. The pressure balance equation, therefore, becomes

$$\Delta P_{vm} + \Delta P_{th} = \Delta P_{vel} + \Delta P_c + \Delta P_{rb} + \Delta P_{wd} + \Delta P_{rd} + \Delta P_{bend1} + \Delta P_{bend2} \quad (18)$$

Unknowns in the pressure balance equation are the air mass flow rate and density. These factors are dependent on the heat transfer process in the system. The temperature of the heated air in the collector, T_c , can be computed from the useful energy collected by the collectors. From Duffie and Beckman (1980),

$$Q_u = A_c F_r [S - U(T_i - T_{amb})] \quad (19)$$

where

Q_u = useful solar energy collected, MJ

F_r = heat removal factor,

S = effective solar radiation incident to collector,

U = overall heat loss coefficient, $W/(m^2K)$,

T_i = inlet air temperature, K and

T_{amb} = ambient temperature, K.

Therefore, the temperature of the heated air is

$$T_c = T_i + Q_u / m C_p \quad (20)$$

During operation, the rockbed was assumed to be continually either charging or discharging. To simplify the dynamic analysis of the rockbed temperature distribution, the bed was assumed to consist of thin horizontal layers (Mumma and Marvin, 1976). The layer immediately after the collector was heated by air at temperature T_c . The rate of heat lost by the air equalled the heat transferred to the rocks plus the heat losses from the walls of the holding structure,

$$mC_{p,a}d\Gamma = h_v A_{rb} dx (T_{tb} - T_c) + U(T_c - T_{amb}) \quad (21)$$

where

$$\begin{aligned} C_p &= \text{specific heat, J/(kg K),} \\ d\Gamma &= \text{temperature increment, K,} \\ dx &= \text{rockbed depth increment, m,} \end{aligned}$$

and the other variables as previously defined.

The equation for the volumetric heat transfer coefficient, h_v , is given by Lof and Hawlyc (1948) as

$$h_v = 279.6 (G/D_r)^{0.7} \quad (22)$$

where

$$\begin{aligned} G &= \text{massflow rate, kg/(m}^2\text{h),} \\ D_r &= \text{diameter of individual rock, mm, and} \\ A_{rb} &= \text{cross sectional area of the rockbed normal to flow, m}^2. \end{aligned}$$

Neglecting the heat losses through the holding structure, Equation 21 can be rearranged and integrated to yield the equation for the temperature of the air after passing through a rockbed layer, n , which is

$$T_{a,n+1} - T_{b,n} = \exp(-h_v A_{rb} dx / mC_{p,a}) (\Gamma_{a,n} - T_{b,n}) \quad (23)$$

The temperature of the storage bed layer, $T_{b,n}$ at any time can be found by equating the heat lost by the air flowing through the bed and the heat gained by the rocks in the layer. In finite difference form (Jansen, 1985)

$$\begin{aligned} mC_{p,a}(T_{a,n} - T_{a,n+1}) \Delta t = \\ (p_b A_{rb} \Delta t)(1 - e)C_{p,b}[T_{b,n}(t + \Delta t) - T_{b,n}(t)] \quad (24) \end{aligned}$$

where

$$\begin{aligned} t &= \text{unit time} \\ p_b &= \text{density of the rock bed, kg/m}^3, \\ e &= \text{fraction of voids in the rockbed} \end{aligned}$$

and the other parameters as previously defined.

The temperature of the layer, n , at any time $t + \Delta t$ may then be written as

$$T_{b,n}(t + \Delta t) = [mC_{p,a}(T_{a,n} - T_{a,n+1})\Delta t / \rho_b A_b \Delta x + (1 - c)C_{p,b}] + T_{b,n}(t) \quad (25)$$

Air coming from the last rockbed layer passes through the wall and roof ducts before it is finally exhausted by the vortex machine. Air temperature changes in response to heat gained/lost by the walls and roof. To quantify the amount of energy gained or lost, the concept of sol-air was adapted. Sol-air temperature is an equivalent temperature of the outside air which, in the absence of all radiation exchanges, would provide the same rate of heat transfer to the exposed surfaces as would exist with the actual combined effects of the incident solar radiation, radiant energy exchange with the sky and other surroundings, and convective heat exchange with the outdoor air (McQuiston and Parker, 1982). Therefore,

$$T_{sa} = T_{amb} + (0.053)I_t - e \Delta R / h_o \quad (26)$$

where

T_{sa} = sol-air temperature, C,

I_t = total solar radiation incident to surface, W/m^2 ,

e = emittance of the surface,

ΔR = difference between the longwave radiation incident on the surface from the sky and the radiation emitted from a blackbody at outdoor air temperature, W/m^2 , and

h_o = coefficient of heat transfer by longwave radiation and convection at the outer surface, W/m^2 .

The constant 0.053 represents the ratio of the absorptance for solar radiation to the coefficient of heat transfer by longwave radiation and convection at the outer surface of the black wall and roof, and $-e \Delta R / h_o$ is the longwave correction factor which is -1 for a nearly vertical wall and -3 for a nearly horizontal roof.

The heat gained/lost by the wall, therefore, is

$$Q_w = (A_w / R_w) (T_{sa,w} - T_{amb}) \quad (27a)$$

where

A_w = area of the wall, m^2 , and

R_w = total solar resistance of the wall, $m^2 \cdot C / W$.

Similarly, for the roof,

$$Q_r = (A_r/R_p)(T_s - T_{amb}). \quad (27b)$$

The temperature of the air in the wall and roof ducts become

$$T_{a,w} = T_{a,n+1} + (Q_w/mC_p) \quad (28a)$$

$$T_{a,r} = T_{a,w} + (Q_r/mC_p) \quad (28b)$$

where

$$T_{a,n+1} = \text{temperature of the air after passing through the rockbed, } C, \text{ and}$$

$$m = \text{air massflow rate, kg/s.}$$

The Program

The program was written in BASIC and was essentially that of pressure and heat balances. The general procedure is shown in Figure 3.

The program is interactive and the user must input the latitude of the area where the facility is located; the dimension, slope (inclination), orientation, and thermal characteristics of the solar collector, walls and roof; the dimension and properties of the rockbed heat storage; and the starting and ending times and dates of the period to be simulated.

There are three subroutines in the program. The first computes necessary solar variables (equation of time, geometric factor, incident radiation, and absorbed solar energy). The second subrouting computes useful solar energy collected by the collectors and heat gained/lost by the walls and roof, and the temperature profile of the rockbed. The third calculates temperatures and massflow at each point in the pressure balance loop. Since temperature (and consequently, densities) and massflow are interdependent, an initial massflow was assumed and an iterative procedure was implemented using a personal computer. To facilitate faster convergence of the pressure balance equation, the Newton-Raphson iteration technique was used. Each iteration was completed when the resulting massflow was within the set accuracy of 0.0001 kg/s. For each run, temperatures of the rockbed, curing air and roof were initialized to be equal to the ambient temperature.

The program can be implemented for all locations where meteorological data such as solar insolation, ambient temperature, relative humidity, and wind velocity are available. For this study, the program was implemented using the 1985 meteorological data taken from Florence, South Carolina.

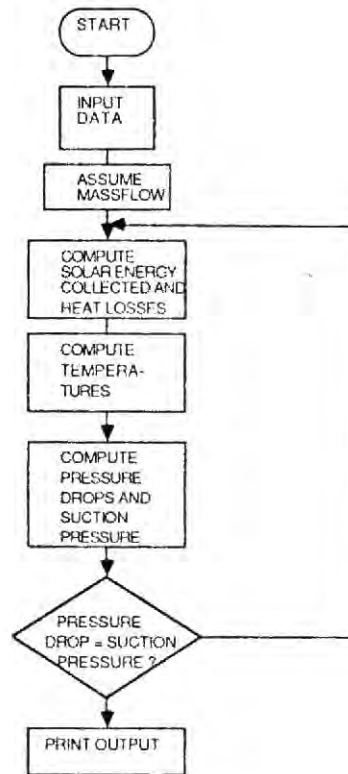


Figure 3. General procedure of the simulation .

Results and Discussion

The pressure to massflow characteristics of the system is shown in Figure 4. The suction pressure generated by thermal bouyancy and the vortex machine in response to the ambient wind velocity is shown in Figure 5. The corresponding massflow is shown in Figure 6. Both the suction pressure and the massflow fluctuated in direct response to wind velocity. During the day, the total motive force was generated almost solely by the vortex machine. This is expected because the observed static pressure drop in the vortex core was very large, 4.9 times that of the dynamic pressure of the wind velocity. Hence, the effect of wind on the total suction pressure was amplified several times. The low contribution of the thermal effects also points to the inadequacy of natural convection alone to provide the needed draft.

With wind velocity ranging from 0.3 to 4.7 m/s for the test period, the maximum suction pressure developed was 66.2 Pa. The resulting massflow ranged from 0.1 to 1.7 kg/s.

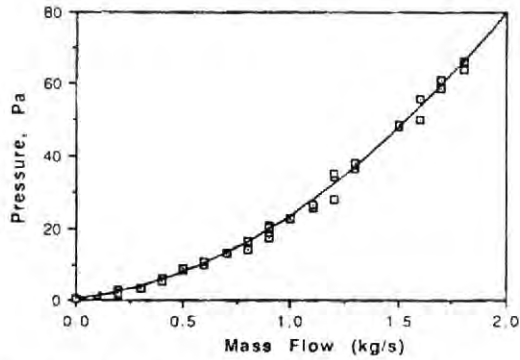


Figure 4. The pressure to massflow characteristics of the system.

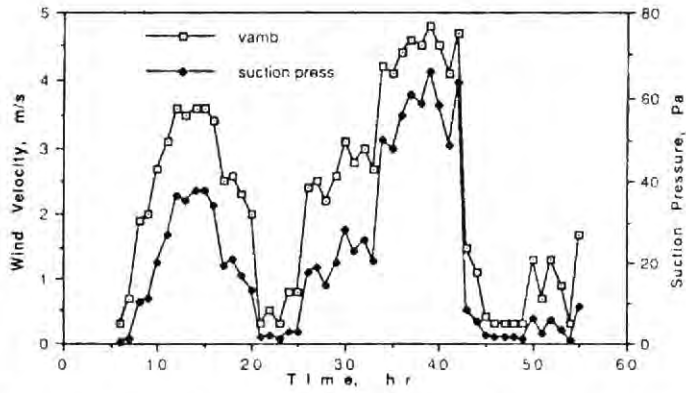


Figure 5. Suction pressure developed in the system relative to ambient wind velocity.

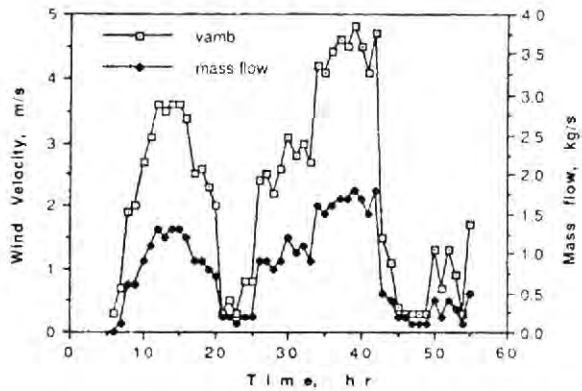


Figure 6. Massflow generated in the system relative to ambient wind velocity.

The generated massflow was sufficient to effectively charge the rockbeds as shown in Figure 7. The combination of low solar radiation and low massflow during the early morning hours (6:00 to 9:00 am) resulted in relatively slow charging. However, as both were increase, charging proceeded quickly. The beds were fully charged at around 2:00 pm.

During the night, when the wind is slow and the rockbed is discharging, the suction pressure due to thermal bouyancy becomes significant. Figure 8 shows this condition taken from the results during the second night. However, the total suction pressure developed was quite low, with a maximum of only 8.4 Pa. The resulting massflow was 0.08 kg/s while the temperature ranged from 29.48 to 45.97 C. Nevertheless, this low flow but relatively high temperature air can still be useful in slow but regulated drying typical in the yellowing phase of tobacco curing.

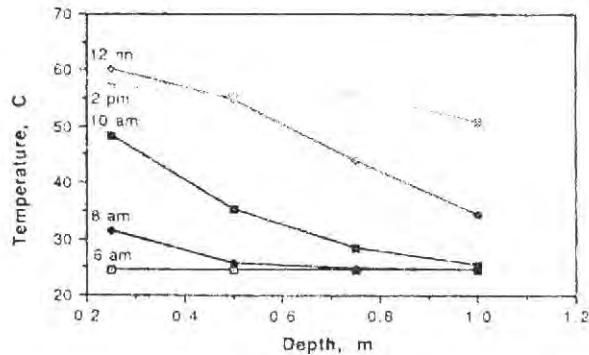


Figure 7. Temperature propagation in the rockbed during charging.

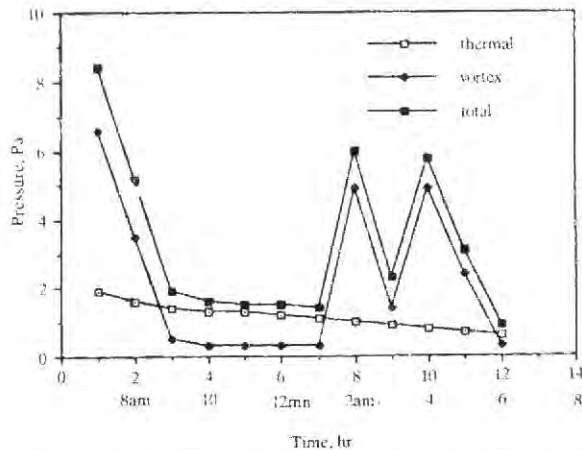


Figure 8. Thermal and vortex generated suction pressure during night time showing the contribution of thermal effect.

To take advantage of the effectiveness of the vortex machine in charging the rockbed and to circumvent its limitation in the discharging process (due to slow winds at night time), it is best adapted for hybrid systems. The vortex machine can free the blower during the charging mode and can compliment it during the discharging mode.

The overall predicted thermal performance of the system is summarized in Figure 9. Under the present scheme of unregulated airflow, the temperature of the heated air from the rockbeds was higher than the ambient, except during the charging hours of the first day. However, the temperature of the air from the collector during these times was much higher than the ambient. Thus, if part of the air from the collector is allowed to enter directly into the chamber, a condition whereby the temperature in the drying chamber is always higher than the ambient can be maintained throughout the day. During the night, the rockbeds can maintain the temperature of the system above ambient temperature. The skewed shape of the heated air graph, however, suggests low flows developed during the night. The rockbeds were fully discharged at 7:00 am. The total energy collected by the system during the 13-hr solar radiation period for July 1, 1985 was 718 MJ while for the next day, it was 979 MJ (Figure 10).

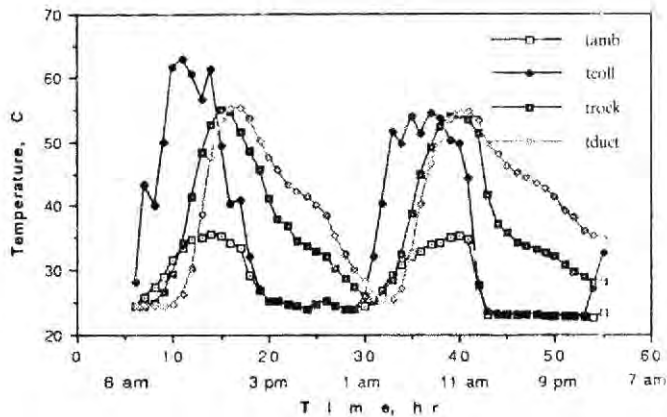


Figure 9. The predicted thermal performance of the system.

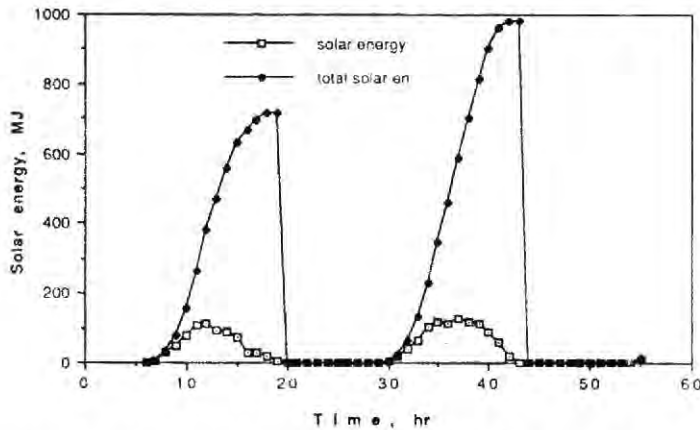


Figure 10. Hourly and total useful energy collected by the system.

Conclusions and Recommendation

The computer simulation program can predict the thermal performance of the solar-aided tobacco curing barn. Based on the results, the vortex machines can theoretically be used as an effective passive charging device for a rockbed solar heat storage system. However, field tests should be conducted to verify the results.

Literature Cited

1. Castro, R. C., J.A. Dulay, A. T. Austria, F.R. Recta, Jr., A.D. Glova and E. M. Dilla. 1985. Design and Development of a Low-cost Solar-aided Flue Curing Barn. Paper presented during the National Symposium on Renewable Energy Technologies, November 5-7, Manila, Philippines. 30 pp.
2. Duffie, J. A. and W. A. Beckman. 1980. *Solar Engineering Thermal Processes*. Wiley and Sons, New York, NY. 762 pp.
3. Jansen, T. J. 1985. *Solar Energy Technology*. Prentice Hall, Inc., Englewood Cliffs, NJ. 205 pp.
4. Lof, G.O. and R. W. Hawley. 1948. Unsteady state heat transfer between air and loose solids. *Industrial and Chemical Engineering*. 40(6): 1061-1070.
5. Mc Quiston, F. C. and J. D. Parker. 1982. *Heating, Ventilating and Air Conditioning. Analysis and Design*. John Wiley and Sons, New York, NY. 653 pp.
6. Mumma, S. A. and W. C. Marvin. 1976. A method of simulating the performance of a pebble bed thermal storage and recovery system. ASME Paper 76-HT, ASME, New York, NY.
7. Shewen, E. C. and K. G. T. Hollands. 1978. Optimization of the flow passage geometry in solar air heaters. Proceedings of the Solar Energy Society of Canada, Inc., London, Ontario.
8. Vered, G. and A. V. Sebald. 1981. Design and control trade-offs for rockbins in passively heated homes with high solar fractions. *Solar Engineering-1981. Proceedings of the American Society of Mechanical Engineers Solar Energy Division 3rd Annual Conference of Systems Simulation, Economic Analysis and Solar Heating and Cooling: Operational Results*.